Atlantic Multidecadal Variability modulates the climate response to El Niño-Southern Oscillation in Australia

Paloma Trascasa-Castro[1], Amanda Maycock[1], Yohan Ruprich-Robert[2], Marco Turco[3] and Frederic Castruccio[4]

[1]University of Leeds, UK [2]Barcelona Supercomputing Center, Spain [3]Universidad de Murcia, Spain [4]National Center for Atmospheric Research, USA

ee17pt@leeds.ac.uk @PTrascasaCastro

Background

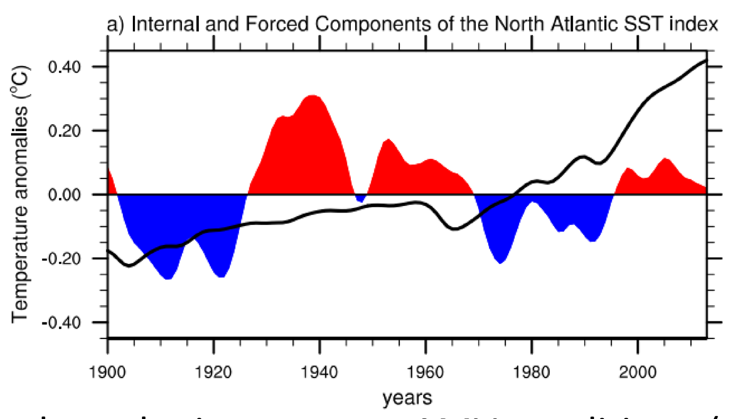

The Atlantic Multidecadal Variability (AMV) is a North-Atlantic basin wide sea surface temperature (SST) fluctuation on multidecadal timescales.

FIG. 1. Internal (red and blue) versus external (black) components of the observed AMV (Ruprich-Robert *et al.*, 2017).

In boreal winter, warm AMV conditions (AMV+) drive tropical Pacific cooling (Fig. 2a), a northward shift of the Intertropical Convergence Zone (ITCZ) and a strengthening of the trade winds across the equatorial Pacific Ocean (Fig. 2b). These changes in the tropical Pacific mean state are a signature of a strengthened Walker circulation, a key mechanism in the tropical Pacific response to warm SSTs in the tropical/North Atlantic at interannual (Rodríguez-Fonseca *et al.*, 2009) and multidecadal (Ruprich-Robert *et al.*, 2017) timescales.

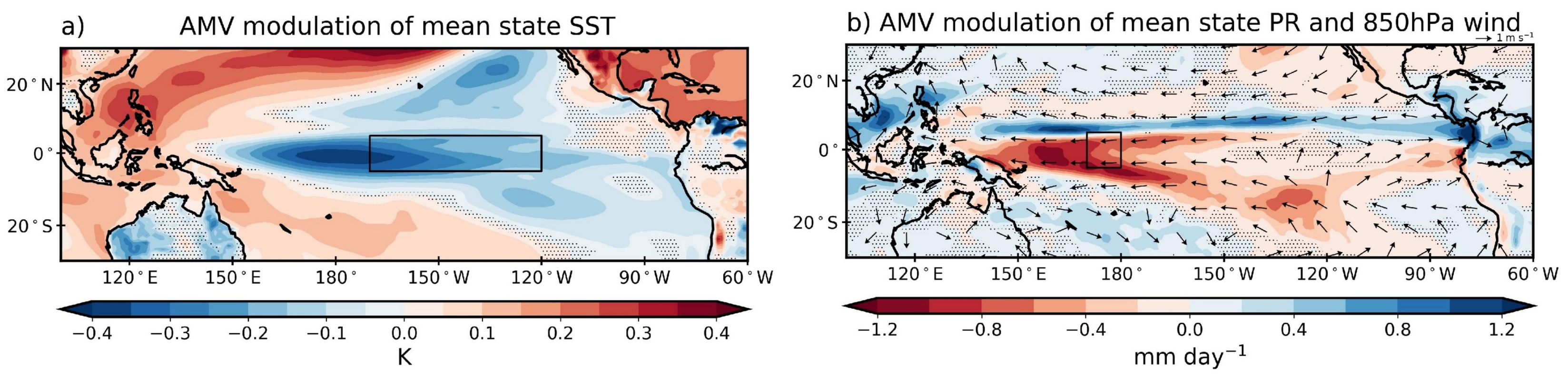

FIG. 2. Tropical Pacific mean state changes between Atlantic Multidecadal Variability (AMV)+ and AMV− in (a) SST(b) precipitation and 850 hPa winds in boreal winter (December-February; DJF). Note inverted color bars in the left and right columns. Hatched areas show non significant anomalies at the 95% confidence level.

Methods

Does AMV modulate ENSO variability? How?

We used output of idealized AMV simulations run with the NCAR-CESM1 model as part of the Decadal Climate Prediction Project (DCPP) (Boer *et al.* 2016). The Observed AMV pattern (ERSSTv4) was imposed to preindustrial SSTs through **surface flux restoring.**

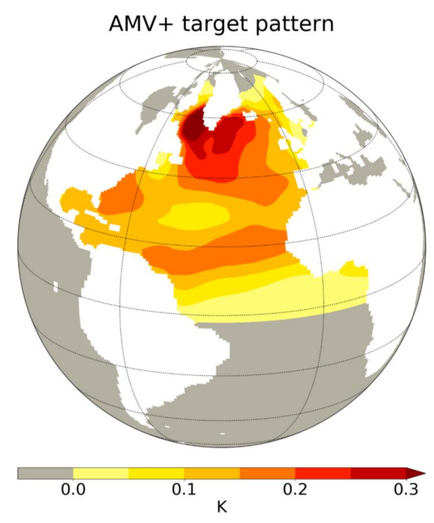

Fixed AMV pattern which does not vary in time nor account for AMV seasonality. 30 members x 9 full winter seasons = 270 years per AMV phase.

FIG. 3. AMV+ target pattern obtained from observations (ERSSTv4). Filled contours correspond to SST anomalies (K) warm AMV phase. The negative AMV pattern (AMV-) is equivalent in amplitude but with opposite sign SST anomalies.

AMV modulation of El Niño*→

* Same method for La Niña

El Niño impacts in AMV+ – El Niño impacts in AMV-

$$(\text{El Niño}_{AMV+} - \mu_{AMV+}) - (\text{El Niño}_{AMV-} - \mu_{AMV-})$$

AMV+ damps ENSO variability…

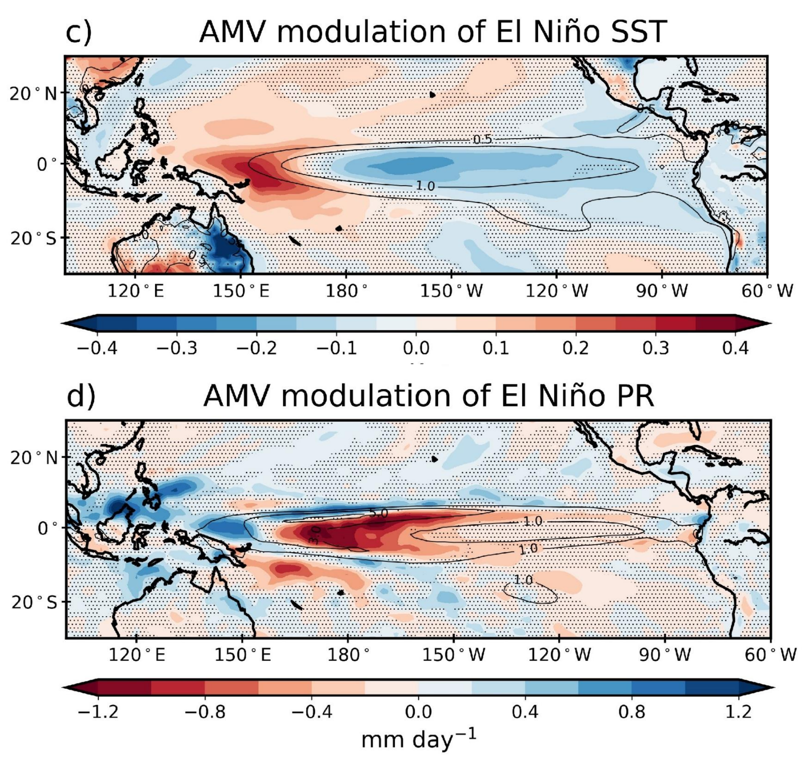

El Niño events in AMV+ have cooler SSTs **(~10%)** in the central (CP) and eastern (EP) equatorial Pacific and warmer SSTs in the west (WP) Pacific (Fig 4.a).

Under AMV+ conditions, precipitation anomalies during El Niño (Fig. 4.b) shift from CP to WP, with a **decrease in CP precipitation anomaly of ~40%**.

FIG. 4. AMV modulation of El Niño (c) SST and (d) precipitation. Black contours show composite El Niño anomalies from AMV− overlaid in contours.

To find the cause of the change in ENSO SSTs between AMV+ and AMV- we used the Bjerknes Stability index (BJ) (Jin *et al.* 2006).

Current damping | Thermodynamic | Zonal advective | Ekman | Thermocline

$$2BJ = -\left[a_1\frac{\langle\Delta\bar{u}\rangle_E}{L_x} + a_2\frac{\langle\Delta\bar{v}\rangle_E}{L_y}\right] - [\alpha_s] + \left[\mu_a\beta_u\langle-\frac{\partial\bar{T}}{\partial x}\rangle_E\right] + \left[\mu_a\beta_w\langle-\frac{\partial\bar{T}}{\partial z}\rangle_E\right] + \left[\boldsymbol{\mu_a\beta_h}\langle-\frac{\bar{\boldsymbol{w}}}{\boldsymbol{H_1}}\rangle_E\,\boldsymbol{a_h}\right]$$

ENSO growth rate decreases by 30% in AMV+ compared to AMV-

… by weakening the thermocline feedback

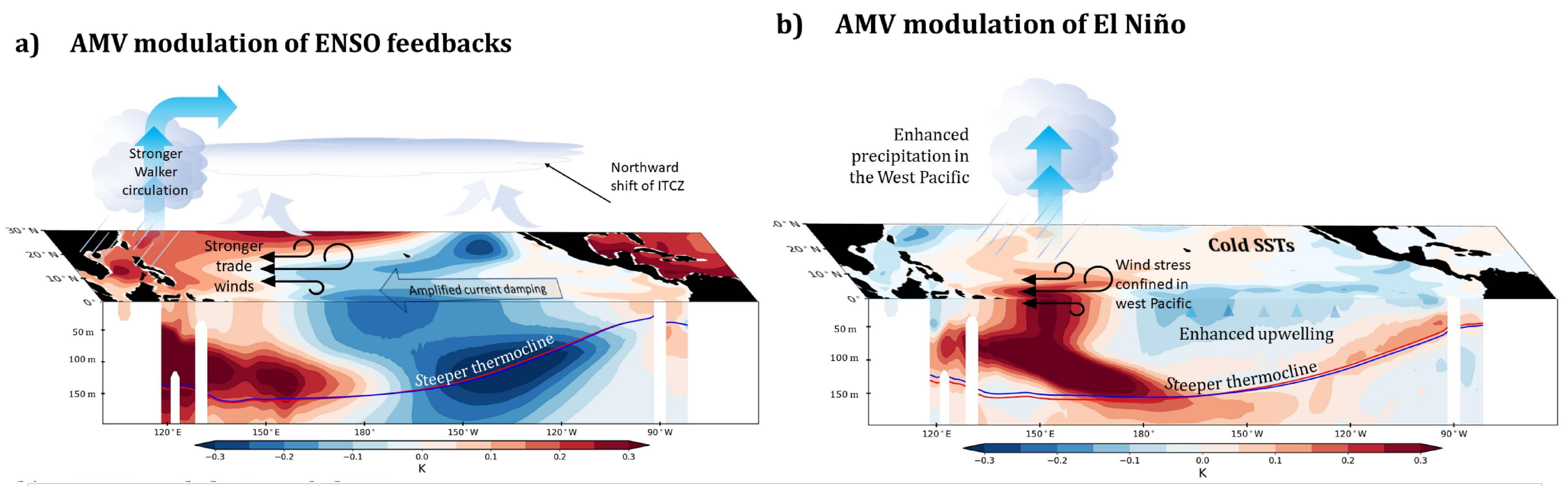

FIG. 5. Schematic overlay of (a) the mean state changes due to AMV in the equatorial Pacific in JASON and (b) the climate response to El Niño modulated by the AMV in DJF. Shading shows ocean temperature anomalies. Red and blue lines in both panels show the 20°C isotherm in the AMV+ and AMV− experiments, respectively.

The main contributor to the decrease in ENSO growth rate is a **weakened thermocline feedback,** which dominates from boreal summer through early winter, directly affecting the ENSO growing season.

During AMV+ (Fig. 5a), equatorial wind stress anomalies are confined over the WP, making the EP thermocline less sensitive to wind stress (↓$\boldsymbol{\beta_h}$, in agreement with Lübbecke and McPhaden (2014)). The East-West upper ocean heat content gradient increases and the thermocline steepens in AMV+ compared to AMV-.

The trade wind slackening associated with El Niño are accompanied by a westward shift of the maximum SST and deep convection anomalies (Fig. 5b).

AMV modulation of ENSO impacts in Australia

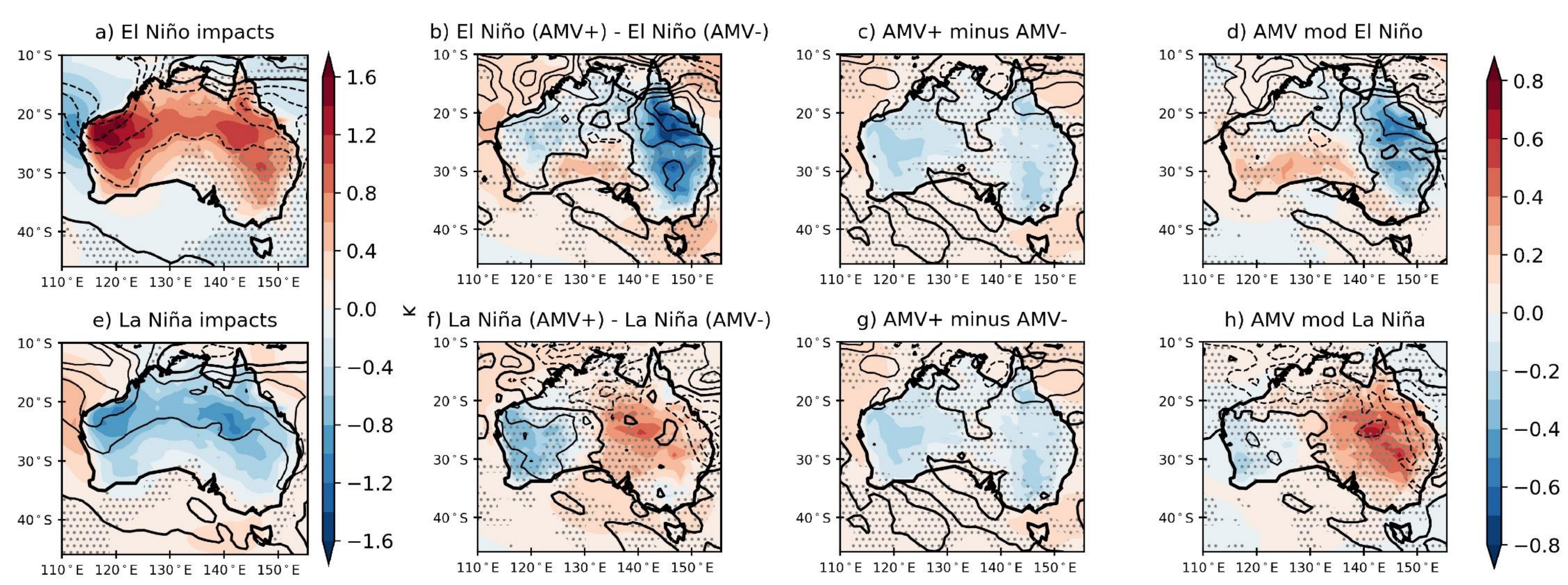

FIG. 6. El Niño (top) and La Niña (bottom) temperature anomalies (K) in filled contours and precipitation anomalies (mm day^{-1}) in black contours in DJF. Mean ENSO impacts are shown in a) and e), the difference between the absolute response to El Niño or La Niña in AMV+ and AMV- is shown in b) and f), the mean changes due to AMV appear in subpanels c) and g) and the AMV modulation of El Niño or La Niña impacts are shown in d) and h).

Over **Eastern Australia** and under warm AMV conditions, El Niño summers are cooler and wetter, and La Niña summers are hotter and drier → AMV **weakens** ENSO impacts.

Over **Southwest Australia**, El Niño summers are hotter and drier and La Niña summers are cooler and wetter in AMV+ compared to AMV- → AMV **intensifies** ENSO impacts.

We linked the surface response to anomalous subsidence associated with changes in large scale dynamics driven by AMV+, rather than caused by local scale processes.

ENSO-driven burned area in SE Australia

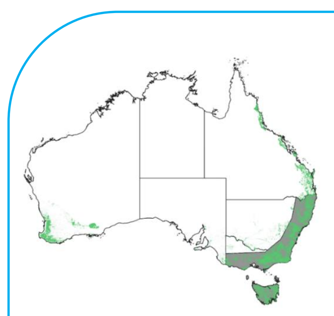

FIG 7. Study domain consists of largely forested areas in the southeast of Australia with fire data from 1971 to 2020.

Empirical relationship based on the observed standardized precipitation and evapotranspiration index (SPEI) estimates the extent of burned area based on preconditioning factors such as changes in precipitation and temperature prior and during the fire season.

$SPEI_{12\ (Feb\text{-}Jan)}$ explains **66%** of observed burned area in SE Australia.

observations ⇨ $\log[BA(t)] = \beta 1 + \beta 2 \cdot SPEI(t)_{sc,m} + \varepsilon(i,t)$ ⇨ CESM1 output

AMV and ENSO superimposed

El Niño + AMV+ → ↓ burned area

AMV signal removed

El Niño − μ AMV → ↓ burned area — Not statistically significant

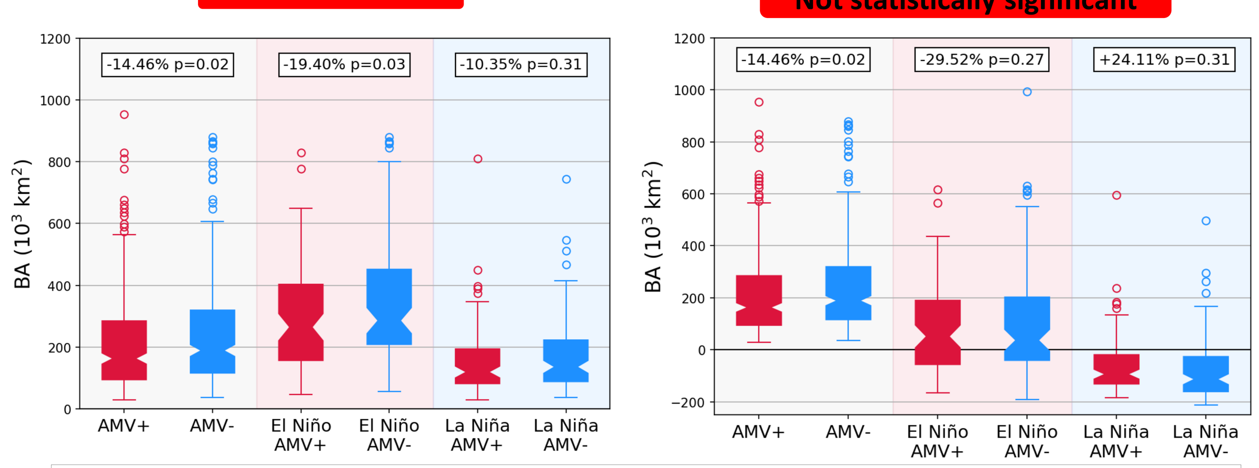

FIG 8. Boxplots of absolute (left) and anomalous (right) burned area (km^2) in SE Australia estimated using CESM1 output with the empirical SPEI-BA relationship. Red (blue) boxplots indicate values in AMV+ (AMV-). Numbers on top show the % difference between El Niño (or La Niña) in AMV+ and AMV- and their associated p value estimated with a double-sided t-test.

Burned area decreases by 14% in AMV+ compared to AMV-.

When El Niño co-occurs with AMV+, burned area decreases significantly by 19% (Fig. 8 left).

However, if we remove the mean AMV signal we find that there's no statistically significant AMV modulation of the ENSO-fire relationship in SE Australia (Fig. 8 right).

References

Boer, G. J., Smith, D. M., Cassou, C., Doblas-Reyes, F., Danabasoglu, G., Kirtman, B., et al. (2016). The Decadal Climate Prediction Project (DCPP) contribution to CMIP6. *Geoscientific Model Development*, **9**,

Jin, F. F., Kim, S. T., & Bejarano, L. (2006). A coupled-stability index for ENSO. *Geophysical Research Letters*, **33**, L23708.

Lübbecke, J. F., & McPhaden, M. J. (2014). Assessing the twenty-first-century shift in ENSO variability in terms of the Bjerknes stability index. *Journal of Climate*, **27**, 2577– 2587.

Rodríguez-Fonseca, B., Polo, I., García-Serrano, J., Losada, T., Mohino, E., Mechoso, C. R., & Kucharski, F. (2009). Are Atlantic Niños enhancing Pacific ENSO events in recent decades? *Geophysical Research Letters*, **36**, L20705.

Ruprich-Robert, Y., Msadek, R., Castruccio, F., Yeager, S., Delworth, T., & Danabasoglu, G. (2017). Assessing the climate impacts of the observed Atlantic multidecadal variability using the GFDL CM2.1 and NCAR CESM1 global coupled models. *Journal of Climate*, **30**(8), 2785– 2810.

Trascasa-Castro, P., Ruprich-Robert, Y., Castruccio, F., & Maycock, A. C. (2021). Warm phase of AMV damps ENSO through weakened thermocline feedback. Geophysical Research Letters, 48(23), e2021GL096149.

UNIVERSITY OF LEEDS
Barcelona Supercomputing Center – Centro Nacional de Supercomputación
NCAR
Natural Environment Research Council
Geophysical Research Letters – Warm Phase of AMV Damps ENSO Through Weakened Thermocline Feedback